

## Isotope Effects in the Specific Heat of Solid Neon<sup>†</sup>

Eugene Somoza\* and Henry Fenichel

*University of Cincinnati, Cincinnati, Ohio 45221*

(Received 30 November 1970)

Specific-heat measurements of <sup>20</sup>Ne and <sup>22</sup>Ne are reported in the temperature range 2.5–23.5 K. The measurements were made simultaneously on the two isotopes in a calorimeter employing a mechanical heat switch. The results are presented in the form of tables of smoothed values of the following thermodynamic properties: specific heat at constant pressure, specific heat at constant volume, entropy, enthalpy, and the Grüneisen parameter. The results are compared with the Nernst-Lindemann equation, the Grüneisen equation of state, and the theoretical calculations of Barron, Gupta *et al.*, Gillis *et al.*, and Goldman *et al.* Excellent agreement is found at low temperatures between the present results and calculations based on anharmonic models. However, discrepancies arise at higher temperatures.

In recent years renewed interest has been shown in the solid-state properties of the noble gases. The first review article on this subject was published in 1957,<sup>1</sup> and since then several others have appeared.<sup>2–6</sup> Interest in the noble-gas solids (NGS) is due mainly to the following factors:

(a) The atoms of these solids have closed electronic shells. Thus, no free electrons or magnetic moments are available to contribute to the thermodynamic properties. The thermodynamic properties of the NGS are, therefore, determined only by lattice dynamics.

(b) The intermolecular forces between NGS atoms are to a good approximation spherically symmetric central two-body forces. The intermolecular potential can then be written in a simple analytic form. And one often uses the Mie-Lennard-Jones potential:

$$\Phi(r) = \frac{\epsilon}{n-m} \left[ m \left( \frac{\sigma}{r} \right)^n - n \left( \frac{\sigma}{r} \right)^m \right], \quad (n > m) \quad (1)$$

where the parameters  $\epsilon$  and  $\sigma$  represent the potential minimum between two NGS atoms and the separation at the potential minimum, respectively.

(c) This class of solids, which consists of Rn, Xe, Kr, Ar, Ne, and He forms a series whose behavior ranges from classical to quantum.<sup>7</sup> The heavier NGS, such as xenon, exhibit classical behavior, while the lighter ones such as neon exhibit quantum behavior.

The rare-gas solids, then, form an ideal testing ground for the study of the various models of lattice dynamics which have been proposed. Due to the fact that the intermolecular potential is pairwise additive and of a simple form, the sums found in lattice dynamical theories can be evaluated and compared with experimental results. In addition, by applying a lattice dynamics theory to various members of the NGS, one is, in effect, able to “turn on” quantum effects and determine at what

point the theory breaks down.

Some of the above statements represent an idealized solid. There is reason to believe, for example, that the intermolecular forces are not completely pairwise additive. Many-body effects may be present. However, it is generally believed<sup>4,8</sup> that they do not play an important role in the thermodynamic properties of these substances. The question of using the empirical Lennard-Jones potential to represent the real potential between two NGS atoms has been the subject of a great deal of discussion. The consensus is that this potential still provides the best source of information about atoms with closed shells, especially in the neighborhood of the potential minimum. The assumption of pairwise additive forces together with the Lennard-Jones potential allows one to make very useful comparisons between the various theories of lattice dynamics and experimental measurements.

We have measured the specific heat at constant pressure<sup>9</sup> of solid <sup>20</sup>Ne and <sup>22</sup>Ne between 2.2 K and the triple point. Neon is a particularly interesting member of the NGS because it exhibits moderate quantum behavior. Theories which are capable of accurately predicting the properties of the heavier NGS may fail when applied to neon. Thus, solid neon provides a more stringent test of lattice dynamical theories. On the other hand, it is simpler than solid helium, and so it may be used as a preliminary stage in the development of a theory with which the thermodynamic properties of all NGS, including solid helium, may be understood.

Earlier measurements of the specific heat of solid-neon isotopes were reported by Clusius *et al.*<sup>10</sup> at temperatures above 8 K. In addition, the specific heat of natural neon (composed of 90.9% <sup>20</sup>Ne, 8.8% <sup>22</sup>Ne, and 0.3% <sup>21</sup>Ne)<sup>11</sup> has been measured independently by two groups.<sup>12,13</sup> The present data will be compared with these previous measurements as well as with the results of various models of

solids and theories of lattice dynamics.

### I. EXPERIMENTAL METHOD

The specific-heat measurements were performed in a modified version of the apparatus described by Shinozaki and Arrott.<sup>14</sup> Two cylindrical calorimeters, constructed of thin-walled tellurium copper (0.018 in. thickness), were incorporated into the cryostat so that the specific heat of <sup>20</sup>Ne and <sup>22</sup>Ne could be measured simultaneously. Soldered to the inside of each calorimeter was a rolled strip of corrugated copper foil which served to distribute the heat to all parts of the sample. When full, each calorimeter held 0.2 mole of solid neon.

The calorimeters were suspended by means of their filling tubes from a copper platform which served as a heat sink. This platform was itself suspended from the top of the vacuum can by three thin-walled stainless-steel tubes. All electrical leads and capillary tubes were thermally anchored to the top of the vacuum can, as well as to the copper platform. The temperature difference between the platform and the calorimeter was monitored by means of a Au-Co-vs-chromel thermocouple. By heating the platform when necessary, its temperature could always be kept very nearly the same as that of the calorimeters. This procedure reduced the flow of heat between these parts, thereby improving the temperature stability of the calorimeters. The initial cooling of the calorimeters was provided by a mechanical heat switch, which was thermally anchored to the top of the vacuum can.

Temperatures were measured with two germanium resistance thermometers<sup>15</sup> of similar characteristics, one attached to each calorimeter by means of GE insulating varnish No. 7031.<sup>16</sup> These thermometers were calibrated simultaneously in the cryostat described above. At temperatures below 4.2 K they were calibrated using the vapor pressure of liquid helium, and the National Bureau of Standards 1958 temperature scale<sup>17</sup> using the calorimeters themselves as vapor-pressure bulbs. Above 4.2 K the calibration was done by means of a helium constant-volume gas thermometer.<sup>18</sup> The helium virial coefficients of Keesom<sup>19</sup> were used. The temperature-resistance data were fitted to the equation given by Ahlers and Macre.<sup>20</sup>

The neon samples were obtained from Mound Laboratories.<sup>21</sup> The following are the purities quoted by the supplier for <sup>22</sup>Ne: 99% <sup>22</sup>Ne in total neon, 99% total neon; <sup>20</sup>Ne: 99.5% <sup>20</sup>Ne in total neon, 99% total neon.

Only 0.14 moles of <sup>20</sup>Ne and 0.18 moles of <sup>22</sup>Ne were available for the experiment; thus it was important to transfer as much of the samples as possible to the calorimeters and to minimize the amount left in the storage tanks. A toeppler pump was used for this purpose. A given amount of the

sample to be measured (usually about 0.01 mole) was first allowed to flow from its low-pressure storage cylinder into a measuring chamber built of precision bore tubing. Here the quantity of gas was found to an accuracy of 0.4% by measuring heights of mercury with a cathetometer. The sample was then transferred to the calorimeter, which was kept at liquid-neon temperature (24.5–27 K). This process was repeated several times until most of the available gas had been measured and transferred to the calorimeter. Towards the end of the filling procedure the pressure of the neon in the storage tank fell to such a low level that it became necessary to use the toeppler pump in order to transfer gas from the storage tank into the measuring chamber. The temperature and pressure of the samples in the calorimeter were carefully monitored during the entire filling process, in order to prevent formation of blocks in the filling lines.

After filling the calorimeters, the temperature of the cryostat was kept at the triple point of neon for several hours while the helium exchange gas which was necessary in the filling process was pumped out of the vacuum can. The samples were then allowed to cool slowly to 4.2 K. Typically it took 6 h for the samples to cool from the triple point to 4.2 K. It was hoped that this slow cooling would cause the neon to solidify into a small number of single crystals with a minimum number of imperfections.

The usual heat-pulse technique was used to measure the specific heat. The voltage across each germanium resistance thermometer was measured with a Guildline<sup>22</sup> model 9160 GD six-dial potentiometer, whose off-balance dc signal was amplified with a Keithley-type<sup>23</sup> 148 nanovoltmeter and fed into a strip-chart recorder. This resulted in a temperature-vs-time graph for each specific-heat data point. By switching the potentiometer from one resistance thermometer to the other, temperature-vs-time plots were obtained simultaneously for both solids. At temperatures below 5 K the combinations of heat leaks and low heat capacity of the samples caused their temperatures to change rapidly with time at different rates. It was much more difficult to carry out simultaneous measurements at these low temperatures, although each sample could be measured individually.

It should be noted that the simultaneous measurement of specific heat as outlined above does not increase the accuracy or sensitivity of the measurements. It was found, for example, that the scatter of experimental points between several runs was no longer than the scatter within a run. The advantage of the simultaneous method is that it allows the measurements to be done more quickly. The gain in accuracy comes about in the simultaneous calibration of the germanium thermometers. Any syste-

matic error will affect both thermometers in the same way and will tend to cancel out.

## II. RESULTS—COMPARISON WITH PREVIOUS MEASUREMENTS

Simultaneous specific-heat measurements of solid  $^{20}\text{Ne}$  and  $^{22}\text{Ne}$  were made in three separate runs in the range 2.2–23 K. The experimental data are given in Tables I and II for  $^{20}\text{Ne}$  and  $^{22}\text{Ne}$ , respectively.<sup>24</sup>

The calculated experimental error below 18 K is 2%. Above 18 K, uncertainties in the temperature given by the gas thermometer resulted in an error of 6%. In addition, at higher temperatures there is a systematic error introduced by the fact that, as the sample is heated, some of the heat goes into vaporizing the solid. This error reaches about 10% at the triple point.<sup>13</sup> We estimate the error in  $\Delta C_p$ , the difference in the specific heat between the two isotopes, to be 8% for temperatures below 18 K, and higher above.

After examining the data we found no systematic differences in the data from different runs. That is, the scatter of experimental points within a run was the same as scatter between several runs. In addition, there was no significant difference in the specific heat when measured in different calorimeters. For these reasons it was felt justified to fit all the data from all runs for each isotope with a polynomial curve. The smoothed  $C_p$  values<sup>9</sup> for  $^{20}\text{Ne}$  and  $^{22}\text{Ne}$  thus obtained are given in Tables III and IV, respectively.

Using the smooth values of  $C_p$ , we have calculated the specific heat at constant volume  $C_v$  from the relation<sup>25</sup>

$$C_p - C_v = \beta^2 T / \rho \chi_T, \quad (2)$$

where the experimental values for the expansivity  $\beta$ , density  $\rho$ , and isothermal compressibility  $\chi_T$  of Batchelder *et al.*<sup>26,27</sup> have been used. In addition, the entropy  $S$  and the enthalpy  $H$  have been calculated by direct integration of the  $C_p$  data. Smoothed values of these quantities appear in Tables III and IV. These tables also include the Grüneisen parameter  $\gamma$  of each isotope as a function of temperature. This was calculated from the expression<sup>25</sup>

$$\gamma = \beta / \rho \chi_T C_v. \quad (3)$$

The present results may be compared with the previous isotope measurements of Clusius *et al.*<sup>10</sup> and with recent natural-neon measurements.<sup>12,13</sup> We find that our measurements are generally 6% higher than those of Clusius *et al.* We cannot find any reason for this; however, since our  $^{20}\text{Ne}$  data are in good agreement with the natural-neon measurements of Fenichel and Serin<sup>12</sup> and of Fagerstroem and Hollis-Hallett<sup>13</sup> we feel that our calorimetry techniques are sound. When the differences

TABLE I. Measured specific heats of solid  $^{20}\text{Ne}$ .

$T$ (K)	$C_p$ (J/mole K)	$T$ (K)	$C_p$ (J/mole K)
Run 1 (0.0889 mole)			
2.235	0.0572	4.691	0.6045
2.377	0.0713	4.795	0.6431
2.395	0.0697	4.799	0.6326
2.404	0.0713	4.872	0.7036
2.469	0.0769	4.916	0.6929
2.552	0.0879	5.046	0.7503
2.559	0.0863	5.053	0.7628
2.702	0.1020	5.201	0.8522
2.745	0.1125	5.463	1.019
2.878	0.1234	5.716	1.198
2.920	0.1340	5.854	1.258
3.046	0.1524	6.080	1.452
3.050	0.1467	6.234	1.560
3.090	0.1635	6.369	1.673
3.230	0.1865	6.596	1.859
3.249	0.1898	6.833	2.040
3.348	0.2084	7.199	2.377
3.450	0.2274	7.751	2.877
3.478	0.2364	8.375	3.562
3.512	0.2407	8.777	4.004
3.735	0.2934	9.465	4.558
3.895	0.3583	10.88	6.759
3.899	0.3380	11.74	8.115
3.903	0.3390	12.51	9.036
4.029	0.3798	12.71	9.534
4.245	0.4499	12.97	9.917
4.220	0.4376	13.49	10.80
4.247	0.4524	13.88	10.94
4.388	0.4963	14.52	11.46
4.474	0.5389	15.89	13.47
4.544	0.5441	17.05	15.54
4.547	0.5483	19.57	19.96
4.575	0.5561	21.22	23.46
4.681	0.6020		
Run 2 (0.1084 mole)			
2.798	0.1185	5.855	1.259
2.873	0.1348	6.063	1.403
3.132	0.1669	6.292	1.584
3.224	0.1811	6.514	1.753
3.341	0.2047	6.702	1.890
3.480	0.2319	6.853	2.024
2.746	0.1126	7.166	2.308
2.788	0.1136	7.412	2.535
2.813	0.1184	7.677	2.793
2.835	0.1178	7.973	3.090
2.906	0.1336	8.319	3.475
2.973	0.1360	8.706	3.797
3.026	0.1488	9.056	4.305
3.166	0.1685	9.355	4.718
3.210	0.1784	9.741	5.189
3.301	0.1953	10.18	5.751
3.308	0.1910	10.67	6.431
3.389	0.2130	11.25	7.288
3.396	0.2080	11.62	7.845
3.502	0.2377	12.03	8.566
3.507	0.2320	12.42	9.133
3.546	0.2474	12.84	9.771

TABLE I (continued).

Run 2 (0.1084 mole)			
3.695	0.2826	13.35	10.37
3.839	0.3207	13.69	10.66
4.012	0.3735	14.15	11.46
4.157	0.4486	14.65	12.05
4.315	0.4716	15.90	14.23
4.515	0.5318	16.62	15.07
4.652	0.5864	17.52	16.04
4.753	0.6325	18.34	17.67
4.835	0.6660	19.29	19.28
5.184	0.8340	20.35	21.10
5.330	0.9154	21.93	23.85
5.662	1.129	23.30	26.03
Run 3 (0.1070 mole)			
2.919	0.1259	6.771	1.959
3.068	0.1492	7.229	2.366
3.236	0.1711	7.521	2.614
3.460	0.2117	7.857	2.959
3.582	0.2414	8.094	3.212
3.685	0.2971	8.524	3.678
3.786	0.3114	8.963	4.219
3.877	0.3365	9.517	4.909
4.006	0.3757	9.894	5.393
4.140	0.4169	10.24	5.856
4.337	0.4795	10.45	6.075
4.496	0.5357	10.71	6.386
4.599	0.5642	11.29	7.168
4.714	0.6090	12.07	8.249
4.897	0.6874	12.45	8.821
4.773	0.6252	13.09	9.637
5.054	0.7599	13.46	10.27
5.243	0.8661	13.91	11.05
5.387	0.9467	14.33	11.52
5.547	1.044	15.72	13.40
5.655	1.119	16.46	14.33
5.768	1.191	17.43	16.02
5.964	1.327	18.50	17.95
6.126	1.429	20.09	20.35
6.439	1.687	21.88	23.41

in the specific heats of  $^{20}\text{Ne}$  and  $^{22}\text{Ne}$  are compared (see Fig. 6), the data of Clusius *et al.* and the present data agree to within the combined experimental errors.

In making comparisons between various sets of specific-heat data, it is convenient to compare the Debye temperature  $\Theta^C$  rather than the specific-heat data itself. This is done in Fig. 1 where we present our results together with all other available data. The tables of Giguère and Boisvert<sup>28</sup> were used to convert the specific heat at constant volume to  $\Theta^C$ . The figure demonstrates the large discrepancy between the Clusius work and the present results. The agreement between our  $^{20}\text{Ne}$  curve and the natural neon of Fenichel and Serin is quite good. However, we note that the oscillations in the Debye temperature curve appearing in their data are not

as pronounced in the present result.

In Fig. 2 the Debye temperature is plotted and corrected for thermal expansion. Such a procedure is followed in order to facilitate comparison of the experimental results with the quasiharmonic theory. This is done by reducing the Debye temperature corresponding to the actual crystal volume,  $\Theta^C(V, T)$  to the Debye temperature corresponding to the crystal volume at 0 K,  $\Theta^C(V_0, T)$ . The following relation<sup>29</sup> was used to obtain Fig. 2 from Fig. 1:

$$\Theta^C(V_0, T) = \Theta^C(V, T) \left( \frac{\rho(0)}{\rho(T)} \right)^\gamma. \quad (4)$$

The values of the Grüneisen parameter  $\gamma$  were taken from Tables III and IV and  $\rho$  from Batchelder.<sup>27</sup> In addition to all the other points of Fig. 1, Fig. 2 also includes the natural-neon data of Fagestroem and Hollis Hallet<sup>13</sup> taken from the paper of Batchelder *et al.*<sup>27</sup>

By extrapolating the present measurements to absolute zero, we have calculated the Debye temperature  $\Theta_0^C$  and the sublimation energy  $L_0$  at  $T = 0$  K. We obtain for  $^{20}\text{Ne}$ :  $\Theta_0^C(20) = (74.5 \pm 1.2)$  K and  $L_0(20) = (461 \pm 9)$  cal; and for  $^{22}\text{Ne}$ :  $\Theta_0^C(22) = (71.7 \pm 1.2)$  K and  $L_0(22) = (469 \pm 9)$  cal. These results have been discussed in greater detail elsewhere.<sup>30</sup>

### III. DISCUSSION

In comparing our results with theory we shall restrict the discussion to temperatures below 18 K. The reason for this is that the error in  $C_V$  at high

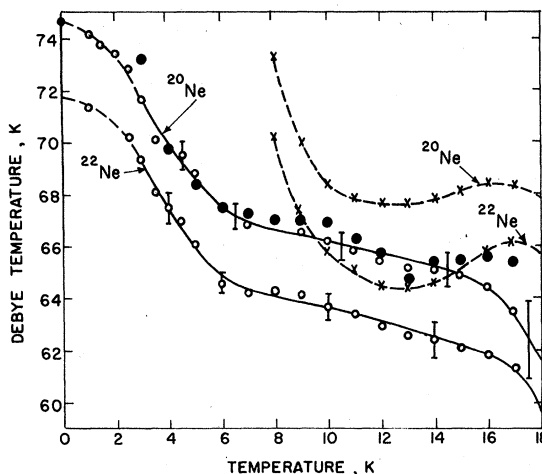


FIG. 1. Experimental temperature dependence of the Debye temperature  $\Theta^C$  reduced from the specific heat at constant volume. o-o: present result; x-x: Clusius *et al.* (Ref. 10); ●-●: natural-neon measurements of Fenichel and Serin (Ref. 12). The extrapolation to 0 K was achieved by fitting the low-temperature points to a parabola. The curves have not been corrected for thermal expansion of the solid.

TABLE II. Measured specific heats of solid  $^{22}\text{Ne}$ .

$T$ (K)	$C_p$ (J/mole K)	$T$ (K)	$C_p$ (J/mole K)
Run 2 (0.0999 mole)			
2.863	0.1453	6.461	1.927
2.910	0.1432	6.636	2.066
3.035	0.1644	6.788	2.230
3.069	0.1800	7.078	2.487
3.148	0.1837	7.338	2.742
3.201	0.1927	7.566	2.965
3.249	0.2141	7.877	3.305
3.286	0.2099	8.188	3.650
3.346	0.2306	8.596	4.178
3.369	0.2293	8.951	4.593
3.426	0.2451	9.257	5.004
3.440	0.2434	9.613	5.503
3.483	0.2548	10.05	6.068
3.489	0.2587	10.54	6.782
3.595	0.2864	11.07	7.554
3.604	0.2876	11.44	8.117
3.729	0.3416	11.82	8.653
3.760	0.3440	12.20	9.299
3.840	0.3613	12.65	9.975
4.027	0.4184	13.08	10.53
4.172	0.4711	13.45	11.07
4.358	0.5424	13.86	11.61
4.534	0.6096	14.33	12.25
4.682	0.6783	14.86	13.19
4.799	0.7193	15.50	13.88
4.909	0.7594	16.26	14.91
5.130	0.9161	17.15	16.29
5.267	1.007	17.95	17.60
5.399	1.108	18.87	19.16
5.541	1.202	19.93	20.96
5.700	1.316	21.47	23.76
5.864	1.438	22.70	26.25
6.255	1.775	23.36	27.19
Run 3 (0.1054 mole)			
2.612	0.0962	6.093	1.614
2.665	0.1040	6.357	1.831
2.725	0.1134	6.712	2.153
2.765	0.1204	7.160	2.589
2.812	0.1297	7.413	2.835
2.916	0.1437	7.767	3.202
3.035	0.1617	8.000	3.468
3.154	0.1828	8.415	3.945
3.262	0.2036	8.839	4.461
3.385	0.2284	9.380	5.179
3.419	0.2424	9.748	5.668
3.511	0.2632	10.09	6.146
3.600	0.2870	10.03	6.393
3.710	0.3165	10.55	6.743
3.853	0.3587	11.12	7.550
3.998	0.4044	11.86	8.642
4.188	0.4736	12.25	9.330
4.345	0.5358	12.84	10.22
4.541	0.6211	13.21	10.83
4.673	0.6681	13.64	11.43
4.882	0.7542	14.02	11.95

TABLE II. (continued).

Run 3 (0.1054 mole)			
4.914	0.7705	14.60	12.69
5.135	0.9183	15.34	13.70
5.229	0.9749	16.06	14.64
5.293	1.015	17.01	16.18
5.478	1.142	18.04	17.75
5.700	1.319	19.59	20.03
5.849	1.425	21.34	23.62
		23.21	28.27

temperatures is considerably greater than at lower temperatures. This large error arises not only from the error in the  $C_p$  data discussed in Sec. II, but is also due to the large error in the measured values of compressibility at high temperatures.<sup>27</sup> In addition to this, at temperatures near the triple point, thermal generation of vacancies in the crystal begins to contribute significantly to its thermodynamics properties.<sup>31</sup> No attempt was made to account for this fact in our data analysis. We estimate that this omission will contribute, at most, an error of 5% at the triple point and a much smaller one for temperatures below 18 K.

#### A. Early Theories

Although, as previously mentioned, the isotopes of neon are expected to deviate significantly from classical behavior, it is of some value to compare the present experimental results with some of the early model theories. This comparison is especially interesting in view of the conclusions of the frequency-shift model of Barron<sup>32</sup> which predicts that in the low-temperature limit the thermodynamic properties of anharmonic crystals as functions of temperature will appear to be like those of harmonic crystals. The temperatures must be low enough and in the range where the zero-point energy is much larger than the thermal energy of the crystal. For neon at the triple point, the zero-point energy is three times the thermal energy, so that the harmoniclike behavior should be noticeable over a large portion of the temperature range of the solid-neon isotopes. This type of comparison was made for argon by Peterson *et al.*<sup>33</sup> It was found that the experimental results for argon were in good agreement with some of the early model theories of solids. It seems, therefore, worthwhile to make the same kind of comparison for the more anharmonic crystals of neon.

One of the early empirical relations is the Nernst-Lindemann equation<sup>25</sup>:  $(C_p - C_v)/C_p^2 T = A$ , where  $A$  is assumed to be independent of temperature. In the case of the neon isotopes it is found to be approximately a constant, varying by only 3% in the temperature range between 5 and 16 K. The

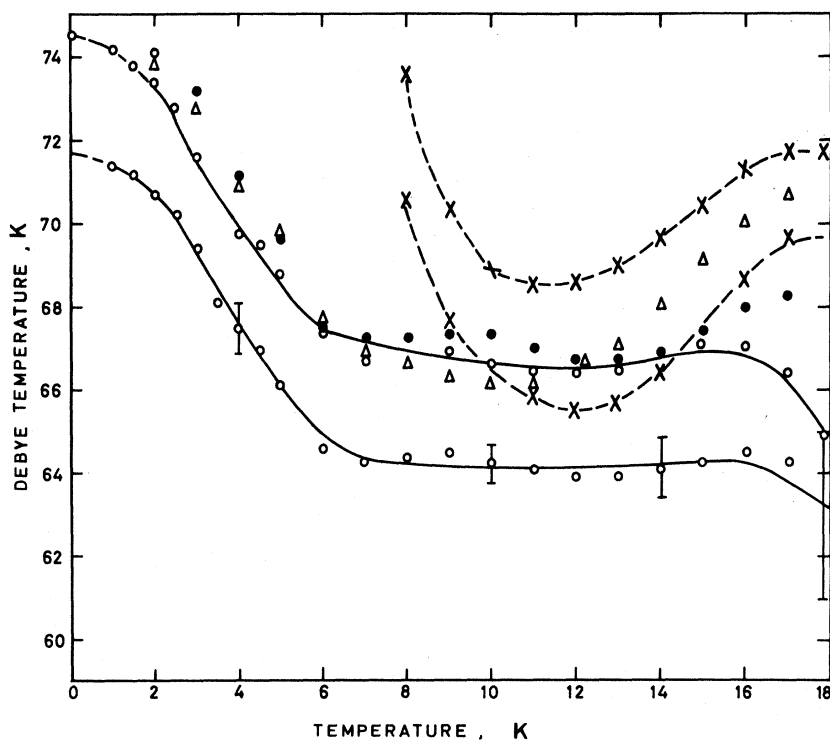


FIG. 2. Temperature dependence of the Debye temperature  $\Theta^C(V_0, T)$ , corresponding to the crystal volume at absolute zero. In addition to the data found in Fig. 1, the natural-neon data of Fagestroem and Hollis Hallet (Ref. 13) is also included ( $\Delta\Delta$ ).

average values of  $A$  in this range are  $A = (49.2 \pm 1.0) \times 10^{-5}$  mole/J for  $^{20}\text{Ne}$  and  $A = (48.5 \pm 2.0) \times 10^{-5}$  mole/J for  $^{22}\text{Ne}$ . There is a drop in  $A$  at low and high temperatures for both isotopes. The low-temperature drop is caused by experimental uncertainties which arise from the fact that  $A$  is proportional to the square of the coefficient of thermal expansion—a quantity which is very difficult to measure accurately at low temperatures. The high-temperature drop in  $A$  is real.

Another early empirical relation we shall discuss is the Grüneisen equation of state. The equation is<sup>34</sup>

$$\frac{V_T - V_0}{V_0} = \frac{E_T}{Q - bE_T}, \quad (5)$$

where  $V_T$  is the molecular volume at temperature  $T$ ,  $V_0$  is the molecular volume at absolute zero, and  $E_T$  is the thermal energy. The constants  $Q$  and  $b$  are given by

$$Q = V_0/\chi_0\gamma_0, \quad (6a)$$

$$b = \frac{1}{6}(m+n+3), \quad (6b)$$

where  $\chi_0$  and  $\gamma_0$  are the absolute-zero values of the compressibility and Grüneisen parameter, respectively. The integers  $m$  and  $n$  are the exponents of the intermolecular potential equation when written in the form

$$V(r) = -Ar^{-m} + Br^{-n}. \quad (7)$$

The thermal energy  $E_T$  has been calculated by graphic integration of  $C_V$ . According to Eq. (5) a plot of  $E_T V_0/\Delta V$  vs  $E_T$  should yield a straight line whose intercept on the vertical axis is  $Q$  and whose slope is  $b$ . This graph has been plotted for the neon isotopes in Fig. 3. In the temperature range 9–18 K, the experimental points do indeed fall along a straight line. The values of  $Q$  and  $b$  obtained from the graph are for  $^{20}\text{Ne}$

$$Q = 5.51 \times 10^3 \text{ J/mole},$$

$$b = 6.67,$$

and for  $^{22}\text{Ne}$

$$Q = 5.66 \times 10^3 \text{ J/mole},$$

$$b = 6.23.$$

The self-consistency of this theory can be checked by calculating the constants  $Q$  from Eq. (6a) and comparing them with the above values. In order to do this the parameter  $\gamma$  has been taken to be 2.78 for both isotopes. This is the value obtained from Fig. 4 if the apparent drop of the curve at low temperatures is ignored. The values of  $V_0$  and  $\chi_0$  are taken from Batchelder *et al.*<sup>27</sup> The results are  $Q = 5.35 \times 10^3$  J/mole for  $^{20}\text{Ne}$  and  $Q = 5.51 \times 10^3$  J/mole for  $^{22}\text{Ne}$ , which are in good agreement with the values of  $Q$  calculated from Fig. 3. In particular the 2.7% difference between  $Q$  of  $^{20}\text{Ne}$  and  $^{22}\text{Ne}$  obtained from Fig. 3 is in excellent agreement with the value 3% obtained using Eq.

(6a) and experimental values of  $V_0$ ,  $\chi_0$ , and  $\gamma_0$ . However, the value obtained from Eq. (6b) for the sum of the exponents appearing in the intermolecular potential equation [Eq. (7)] is 33.4 for  $^{20}\text{Ne}$  and 37.6 for  $^{22}\text{Ne}$ , which are much larger than the value of 18 commonly used for both.

The final empirical relation we shall discuss is also due to Grüneisen. According to this model, there exists a parameter (the Grüneisen parameter  $\gamma$ ) which is a measure of the dependence of the normal frequencies of the crystal on volume. It is related to several thermodynamic quantities of the solid as shown in Eq. (3) and is assumed to be independent of temperature. In Fig. 4 the Grüneisen parameters for the neon isotopes are plotted against temperature. The upper curve gives the results of Clusius *et al.* and the lower curve, the present results. The data of Batchelder *et al.* for  $\beta$ ,  $\rho$ , and  $\chi_T$  have been used. In the range between 5 and 17 K this parameter is essentially temperature independent. The graph also shows no isotopic difference in  $\gamma$ . This is in agreement with the specific-heat experiments of Sample and Swenson<sup>35</sup> who found that  $\gamma$  is isotopically invariant in the solid-helium isotopes. As in the case of the Nernst-Lindemann constant, the present experimental results indicate that the Grüneisen parameter has a very sensitive temperature dependence below 5 and above 17 K. Again the high-temperature drop is real while the drop at low temperatures is caused

by the large uncertainty in the coefficient of thermal expansion and most likely does not represent the true properties of these crystals.

The high-temperature drop of the Grüneisen parameter is in qualitative agreement with theoretical calculations based on the quasiharmonic approximation<sup>36,37</sup> which indicate that the main variation in  $\gamma$  with temperature occurs in the neighborhood of  $0.2\Theta$ . An anharmonic theory has been used recently to determine the temperature dependence of the Grüneisen parameter for the heavier NGS<sup>8,38</sup>; however, such calculations for neon have not yet appeared.

### B. Modern Theories

Most modern theoretical calculations of the thermodynamic properties of solid neon as functions of temperature have employed the quasiharmonic approximation, although recently several anharmonic models have been used. Unfortunately, most theoretical studies have been limited to natural neon. Only one set of calculations for  $^{22}\text{Ne}$  has been published; this is based on the self-consistent phonon model and will be discussed at the end of this section.

In the absence of exact theoretical calculations we have computed theoretical Debye temperature  $\Theta^C$  vs temperature curves for  $^{22}\text{Ne}$  in an approximate manner from existing calculations on natural neon based on the quasiharmonic theory and on the fre-

TABLE III. Smoothed values of some thermodynamic functions of  $^{20}\text{Ne}$ .  $C_p$  is specific heat at constant pressure;  $C_v$  is specific heat at constant volume;  $S$  is entropy;  $H$  is enthalpy;  $\gamma$  is Grüneisen parameter.

$T$ (K)	$C_p$ (J/mole K)	$C_v$ (J/mole K)	$S$ (J/mole K)	$H$ (J/mole)	$\gamma$
3.0	0.143	0.143	0.0527	0.322	0.625
3.5	0.242	0.242	0.0821	0.445	1.848
4.0	0.367 ± 0.007	0.366 ± 0.007	0.122	0.568	2.436 ± 0.216
4.5	0.529	0.528	0.174	0.837	2.706
5.0	0.746	0.744	0.241	1.106	2.759
6.0	1.362 ± 0.027	1.357 ± 0.027	0.427	2.140	2.699 ± 0.150
7.0	2.170	2.154	0.696	3.895	2.686
8.0	3.118	3.079	1.046	6.522	2.741
9.0	4.254	4.173	1.476	10.19	2.746
10.0	5.541 ± 0.111	5.392 ± 0.111	1.990	15.08	2.723 ± 0.213
11.0	6.915	6.659	2.582	21.30	2.754
12.0	8.329	7.922	3.244	28.92	2.782
13.0	9.747	9.137	3.967	37.96	2.824
14.0	11.15 ± 0.17	10.28 ± 0.19	4.741	48.41	2.888 ± 0.276
15.0	12.55	11.36	5.558	60.26	2.901
16.0	13.96	12.43	6.413	73.51	2.864
17.0	15.43	13.54	7.303	88.20	2.738
18.0	17.00 ± 0.23	14.75 ± 0.35	8.229	104.4	2.555 ± 0.284
19.0	18.69	16.11	9.193	122.2	2.302
20.0	20.49	17.61	10.20	141.8	2.037
21.0	22.36	19.38	11.24	163.3	1.661
22.0	24.14	21.05	12.32	186.5	1.390
23.0	25.59	22.34	13.43	211.4	1.211

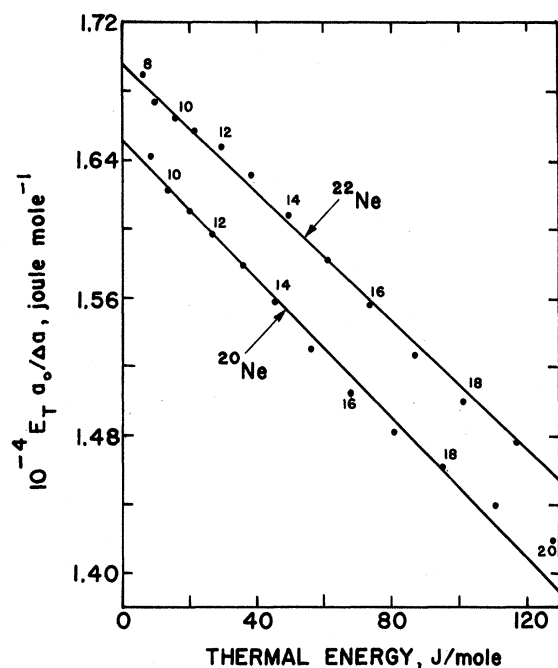


FIG. 3. Test of the empirical Grüneisen equation of state for the solid-neon isotopes. The numbers adjacent to the points on the graph correspond to the temperatures at which the quantities appearing in the Grüneisen equation of state were evaluated.

quency-shift theory of Barron.<sup>32</sup>

The following procedure was used to obtain the theoretical quasiharmonic curve  $\Theta^C$  vs  $T$  for  $^{22}\text{Ne}$ : (a) The quasiharmonic specific-heat values of Leech and Reissland<sup>39</sup> (based on anharmonic potential parameters) obtained from the paper of Batchelder *et al.*<sup>27</sup> were converted to Debye temperatures, using the tables of Giguère and Boisvert.<sup>28</sup> (b) Since

these values of  $\Theta^C$  are based on the quasiharmonic theory, it was assumed that the corresponding values of  $\Theta^C$  for  $^{22}\text{Ne}$  could be obtained from the relation

$$\Theta^C(^{22}\text{Ne})/\Theta^C(^{20}\text{Ne}) = [M(^{20}\text{Ne})/M(^{22}\text{Ne})]^{1/2} = 0.9579, \quad (8)$$

where  $M(^{20}\text{Ne})$  and  $M(^{22}\text{Ne})$  are the molar masses of natural neon and  $^{22}\text{Ne}$ , respectively. That this approximation is plausible may be seen from the fact that this method yields 4.7% for the percent difference between the absolute-zero values of  $\Theta^C$  for the two neon isotopes. This agrees quite well with the value of 4.9% obtained by Barron and Klein<sup>40</sup> using quasiharmonic theory. These quasiharmonic  $\Theta^C$  vs temperature curves for  $^{20}\text{Ne}$  and  $^{22}\text{Ne}$  [labeled  $Q(20)$  and  $Q(22)$ , respectively] are shown in Fig. 5.<sup>41</sup> The same figure also includes the experimental  $\Theta^C$  curves corrected for thermal expansion. These are labeled  $X(20)$  and  $X(22)$ . Note that although the quasiharmonic curves fall well below the experimental ones, their shapes are quite similar. This agrees with the frequency-shift theory of Barron mentioned earlier.

The frequency-shift model of Barron<sup>32</sup> is an anharmonic model which yields numerical results that may be compared with experiment. The analysis is based on the formal anharmonic Born-von Kármán calculations of Leibfried and Ludwig.<sup>42</sup> According to this model the large nonharmonic atomic motions in crystals (due to thermal and zero-point effects) cause a shift in the individual frequencies of the quasiharmonic spectrum. The relative shift is proportional to the total vibrational energy of the lattice. That is,

$$\Delta\nu/\nu = Ae, \quad (9)$$

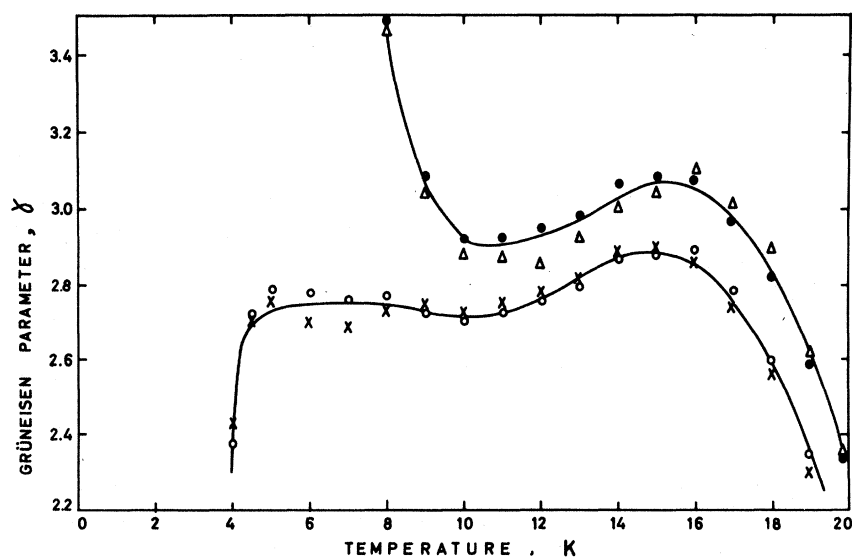


FIG. 4. Temperature dependence of Grüneisen parameter  $\gamma = \beta/\rho C_V \chi_T$ . The lower curve shows the present results for both isotopes.  $\times \times$  is  $^{20}\text{Ne}$  and  $o o$  is  $^{22}\text{Ne}$ . The upper curve shows the results of Clusius *et al.* (Ref. 10).  $\bullet \bullet$  is  $^{20}\text{Ne}$  and  $\Delta \Delta$  is  $^{22}\text{Ne}$ . In all cases the quantities  $\beta$ ,  $\rho$ , and  $\chi_T$  were taken from Batchelder *et al.* (Ref. 27).



TABLE IV. Smoothed values of some thermodynamic functions of  $^{22}\text{Ne}$ .  $C_p$  is specific heat at constant pressure;  $C_v$  is specific heat at constant volume;  $S$  is entropy;  $H$  is enthalpy;  $\gamma$  is Grüneisen parameter.

$T$ (K)	$C_p$ (J/mole K)	$C_v$ (J/mole K)	$S$ (J/mole K)	$H$ (J/mole)	$\gamma$
3.0	0.157	0.157	0.0579	0.353	0.584
3.5	0.264	0.264	0.0901	0.488	1.915
4.0	0.405 ± 0.008	0.405 ± 0.008	0.134	0.623	2.383 ± 0.203
4.5	0.591	0.590	0.192	0.924	2.724
5.0	0.841	0.839	0.266	1.224	2.792
6.0	1.541 ± 0.015	1.534 ± 0.015	0.478	2.395	2.786 ± 0.144
7.0	2.423	2.403	0.780	4.368	2.762
8.0	3.465	3.418	1.168	7.286	2.767
9.0	4.665	4.572	1.643	11.33	2.726
10.0	6.016 ± 0.060	5.848 ± 0.062	2.204	16.66	2.704 ± 0.213
11.0	7.457	7.173	2.844	23.39	2.729
12.0	8.936	8.489	2.556	31.59	2.757
13.0	10.41	9.744	4.330	41.26	2.807
14.0	11.86 ± 0.12	10.91 ± 0.15	5.155	52.40	2.875 ± 0.281
15.0	13.28	12.00	6.022	64.97	2.881
16.0	14.68	13.02	6.923	78.95	2.898
17.0	16.11	14.07	7.856	94.35	2.787
18.0	17.60 ± 0.18	15.21 ± 0.32	8.819	111.2	2.599 ± 0.297
19.0	19.22	16.49	9.813	129.6	2.355
20.0	20.99	17.97	10.84	149.7	2.072
21.0	22.92	19.72	11.91	171.6	1.722
22.0	24.98	21.76	13.03	195.6	1.393
23.0	27.05	23.67	14.18	221.6	1.185

where  $\nu$  is the frequency and  $e$  is the vibrational energy (thermal plus zero point) in units of  $3R$ , the  $R$  being the gas constant. The anharmonic coefficient<sup>43,44</sup>  $A$  can be approximated from the experimental Debye temperature at absolute zero,  $\Theta_0^{\text{exp}}$ . The following equation may be used<sup>32</sup>:

$$\Theta_0^{\text{exp}} = \Theta^h(-3) \left[ 1 + \frac{3}{8} A \Theta^h(2) \right], \quad (10)$$

where  $\Theta^h(-3)$  and  $\Theta^h(2)$  are the low- and high-temperature limits of the Debye temperature obtained from the specific heat in the quasiharmonic approximation. Other methods of evaluating the constant  $A$  may also be used.<sup>45-47</sup> Using our experimental value of  $\Theta_0^{\text{exp}} = 74.5$  K for  $^{20}\text{Ne}$  and the quasiharmonic values of  $\Theta^h(-3)$  and  $\Theta^h(2)$ , obtained from Leech and Reissland, we obtain the value of  $4.8 \times 10^{-3} \text{ deg}^{-1}$  for  $A$ , which is very close to previous estimates.<sup>27,47</sup> However, the value obtained for  $^{22}\text{Ne}$  using  $\Theta_0^{\text{exp}} = 71.1$  K, and the values of  $\Theta^h(-3)$  and  $\Theta^h(2)$  obtained from Eq. (10) and the Leech and Reissland data is  $A = 5.3 \times 10^{-3} \text{ deg}^{-1}$ . This cannot be correct because  $^{22}\text{Ne}$ , being heavier than  $^{20}\text{Ne}$ , should exhibit smaller anharmonic effects and thus have a smaller value of the anharmonic coefficient  $A$ . This small discrepancy is undoubtedly due to the large number of approximations used in these calculations. A study of the range of  $A$  has been made by Batchelder *et al.*<sup>27</sup> for neon. Their conclusion that  $A$  is uncertain by a factor of 2 is still valid.

As a result of the frequency shift given by Eq.

(9), the anharmonic thermodynamic quantities are shifted relative to the corresponding quasiharmonic quantities. In the case of the specific heat it can be shown<sup>4</sup> that the anharmonic specific heat  $C^a(T)$  at temperature  $T$  is related to the quasiharmonic specific heat  $C^h(T')$  at slightly different temperature  $T'$  by the equation

$$C^a(T) = \frac{1 + Ae - AcT}{1 + Ae} C^h(T'), \quad (11)$$

where

$$T' = T/(Ae + 1). \quad (12)$$

The quantity  $c$  is the quasiharmonic specific heat in units of  $3R$ . Thus if the quasiharmonic specific heat is known as a function of temperature, Eqs. (11) and (12) allow one to generate the corresponding anharmonic curves. This was first done by Batchelder *et al.* for natural neon.<sup>27</sup> We have taken the quasiharmonic curves  $Q(20)$  and  $Q(22)$  of Fig. 5 and used them to generate anharmonic Debye temperature curves using Eqs. (11) and (12). These curves are labeled  $B(20)$  and  $B(22)$  in Fig. 5. In obtaining  $B(20)$  and  $B(22)$ , we took the anharmonic coefficient  $A$  to be  $5 \times 10^{-3} \text{ deg}^{-1}$ . Equation (4) was used to refer these curves to the crystal volume at 0 K. We also include in the figure the experimental results of Fagestroem and Hollis Hallet and of Fenichel and Serin. For clarity only the high-temperature data of these experimental curves are

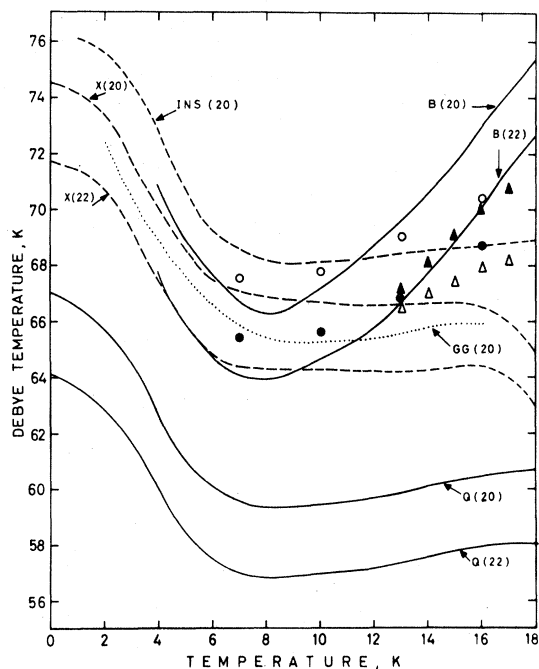


FIG. 5. Comparison of the temperature dependence of the Debye temperature  $\Theta^C$  from various theoretical models and experimental measurements.  $Q(20)$ ,  $Q(22)$ : quasiharmonic calculations of Leech and Reissland (Ref. 39);  $B(20)$ ,  $B(22)$ : frequency-shift calculations;  $GG(20)$ : quasiharmonic calculations of Gupta and Gupta (Ref. 48);  $X(20)$ ,  $X(22)$ : present experimental results;  $INS(20)$ : inelastic neutron scattering calculations of Leake *et al.* (Ref. 52);  $\circ$ ,  $\bullet$ : self-consistent phonon calculations for  $^{20}\text{Ne}$  and  $^{22}\text{Ne}$ , respectively, using a 6-13 model potential (Ref. 51);  $\Delta$ ,  $\blacktriangle$ : represent the experimental data of Fenichel and Serin (Ref. 12) and Fagestroem and Hollis Hallet (Ref. 13), respectively. All curves refer to the crystal volume at absolute zero.

included in Fig. 5. At low temperatures the three sets of experimental data are in good agreement with each other.

It can be seen from Fig. 5 that the theoretical calculations based on Barron's frequency-shift model give a better agreement with experiment than is given by the quasiharmonic theory, especially at low temperatures. Above 9 K, however, the frequency-shifted curves begin to diverge from the experimental curves. The difference in the Debye temperature at  $T=13$  K is 3 K, which corresponds to a 5% difference in specific heat. This difference increases rapidly with rising temperatures. Thus at high temperatures the simple frequency-shift model of Barron tends to underestimate the specific heat. We note, however, that the percent difference in the Debye temperatures of  $^{20}\text{Ne}$  and  $^{22}\text{Ne}$  predicted by this theory does agree with present results quite well throughout the entire temperature range.

Recently some quasiharmonic calculations on natural neon by Gupta and Gupta<sup>48</sup> have appeared in

which a Buckingham intermolecular potential function was used instead of a Lennard-Jones potential. This potential is more satisfactory from a theoretical point of view but has not often been used because of the calculational difficulties involved. The Debye temperature curve for  $^{20}\text{Ne}$  calculated with this model,<sup>41</sup> using anharmonic potential parameters, is shown in Fig. 5 as the curve labeled  $GG(20)$ . This curve is in remarkably good agreement with experiment, even though anharmonic effects have been taken into account only at absolute zero in fixing the potential parameters. Below 10 K this curve deviates more from the experimental curve than does the frequency-shift curve  $B(20)$ , however, above 10 K it keeps the same shape as the experimental curve while the frequency-shift curve diverges. Above 11 K the quasiharmonic curve of Gupta and Gupta is actually in better agreement with experiment than is the anharmonic frequency-shift curve.

It is tempting to try to apply Barron's frequency-shift method described above to the curve of Gupta and Gupta in order to see if it results in even better agreement with experiment. However, this is not possible because when the  $GG(20)$  curve is extrapolated to absolute zero; the resulting value  $\Theta^h(-3)$  so obtained is almost identical with the experimental value  $\Theta_0^{\text{exp}}$ . This causes the anharmonic coefficient, and consequently, the frequency shifts, to vanish.

The excellent agreement between these calculations and experiment leads one to question the usefulness of the Lennard-Jones potential in describing the forces between neon atoms. It is usually tacitly assumed that this potential provides an adequate description of these intermolecular forces, and the reason that satisfactory results are not obtained is blamed on the inadequacy of the dynamical theory rather than on the inadequacy of the Lennard-Jones potential, i. e., on the fact that instead of using a proper anharmonic theory at all temperatures, a quasiharmonic theory is employed with anharmonicity introduced only at absolute zero in the calculation of the potential parameters. The fact that precisely the same dynamical theory with a different intermolecular potential (i. e., the Buckingham potential) yields good results would seem to indicate that it is not the dynamical theory which is at fault.

A very promising anharmonic theory of solids which is currently much in use is the self-consistent phonon model.<sup>49,50</sup> In this model the solid is assumed to consist of a collection of phonons whose frequencies are determined self-consistently. No assumption is made about the smallness of the amplitudes of atomic vibrations. This overcomes the major weakness of the Born-von Kármán theory. An effective Hamiltonian of the harmonic-oscillator form is assumed. The coupling parameters are

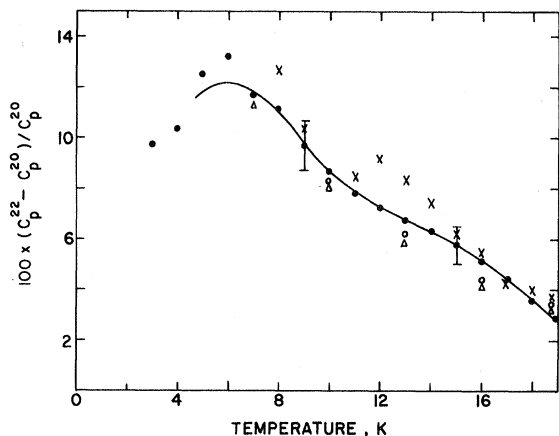


FIG. 6. Isotopic differences in the specific heat at constant pressure for  $^{20}\text{Ne}$  and  $^{22}\text{Ne}$ .  $\bullet$ : present results;  $\times$ : Clusius *et al.* (Ref. 10);  $\circ$ : 6-13 theory of Goldman *et al.* (Ref. 51);  $\Delta$ : 6-12 theory of Goldman *et al.* The solid curve is in a smooth fit of the present data.

left as variation parameters which are determined by minimizing a trial free energy. An iterative process yields the self-consistent frequencies as well as the polarization vector. The calculations have employed a Lennard-Jones intermolecular potential.

The self-consistent phonon model was first used to calculate the thermodynamic properties of the NGS by Gillis *et al.*<sup>49</sup> The results did not agree with the experiments, and, included only  $^{20}\text{Ne}$ . However, improved calculations based on this model have been made by Goldman *et al.*<sup>51</sup> who computed  $C_p$  and  $C_v$  between 7 K and the triple point for solid  $^{20}\text{Ne}$  and  $^{22}\text{Ne}$  using 6-12 and 6-13 model Lennard-Jones intermolecular potentials. It was not possible to extend these calculations below 7 K because the method involves using temperature derivatives of the free energy, which varies very slowly at low temperatures. In order to compare the results of Goldman *et al.* with those discussed earlier, their  $C_v$  values have been converted to Debye temperatures and then corrected for thermal expansion. The 6-13 results are shown in Fig. 5. The open circles correspond to  $^{20}\text{Ne}$  and the closed to  $^{22}\text{Ne}$ . The data derived from a 6-12 potential deviate more from experiment and are not shown on this diagram.

The results of the self-consistent phonon calculation are in good agreement with experiment at intermediate temperatures. However, the shapes of the curves differ from the experimental ones and diverge from them at high temperatures. This divergence is less pronounced than that of the frequency-shift curves  $B(20)$  and  $B(22)$ .

In Fig. 6 we show the isotope effect in the specific heat. The figure includes the calculations of Goldman *et al.*, the present experimental results, and Clusius's data. The agreement between the calcu-

lations of the self-consistent phonon model and present results is very good. Although the 6-13 potential data lie closer to the experimental curve than do the 6-12 data, they are both within experimental error.

Finally, we compare the present work with the inelastic neutron scattering data of Leake *et al.*,<sup>52</sup> who obtained dispersion curves for a single crystal of natural neon in all principal symmetry directions at 4.7 K. The experimental data were represented by smooth curves derived from a force-constant analysis using a Born-von Kármán model. A Mie-Lennard-Jones intermolecular potential model was used, and the analysis was carried out to second- and third-nearest-neighbor approximations. The density-of-states curve which was calculated from the force constants was used to find specific-heat and Debye temperature curves. The Debye temperature curve which results from the second-nearest-neighbor approximation appears in Fig. 5, labeled *INS(20)*. The inelastic neutron scattering curve shows the best agreement with the present experiment. The agreement is quite good throughout the temperature range shown. Above 8 K the two curves are within the experimental error of the present work. At high temperatures the inelastic neutron scattering curve remains flat and does not rise rapidly with temperature as do the theoretical curves of Barron and Goldman *et al.*

#### IV. CONCLUSION

In comparing our experimental results with various theories of lattice dynamics we conclude that purely quasiharmonic theories are not satisfactory. Present anharmonic theories agree much better with experiment, although the results depend greatly on the intermolecular potential used. For example, the introduction of anharmonicity at absolute zero in fixing the intermolecular potential parameters yields results which are in good agreement with experiment only when a Buckingham potential is used. The Mie-Lennard-Jones potential does not give good results in this case. When anharmonicity is included at all temperatures, as in the Barron and self-consistent phonon models, agreement with experiment is good below 14 K when a Mie-Lennard-Jones potential is used. However, at high temperatures (above 14 K) a discrepancy between theory and experiment arises which increases with increasing temperature.

We conclude that existing anharmonic theories are appropriate for the description of the NGS. However, it is likely that better agreement with experiments would result by using an improved potential function rather than the Mie-Lennard-Jones potential. In particular, more calculations using the Buckingham potential in the style of Gupta and Gupta would be most welcome.

## ACKNOWLEDGMENTS

We thank Professor Bernard Goodman for informative discussions, and A. M. Chace and R. Wooley

who constructed the cryostat. We are also pleased to acknowledge Dr. G. K. Horton and Dr. M. L. Klein for their interest in this work and for providing us with their results prior to publication.

†Research supported by the National Aeronautics and Space Administration under Grant No. NGR 36-004-014.

\*Present address: Department of Physics, American University of Beirut, Beirut, Republic of Lebanon.

<sup>1</sup>E. R. Dobbs and G. O. Jones, Rept. Progr. Phys. **20**, 516 (1957).

<sup>2</sup>G. Boato, Cryogenics **4**, 65 (1964).

<sup>3</sup>G. L. Pollack, Rev. Mod. Phys. **36**, 748 (1964).

<sup>4</sup>G. K. Horton, Am. J. Phys. **36**, 93 (1968).

<sup>5</sup>N. R. Werthamer, Am. J. Phys. **37**, 763 (1969).

<sup>6</sup>B. L. Smith, Contemp. Phys. **11**, 125 (1970).

<sup>7</sup>A qualitative measure of the quantum vs classical behavior of a solid is given by the De Boer parameter and the ratio of the zero-point energy to the sublimation energy of the solid. Numerical values for these parameters for neon are given by J. S. Brown, Proc. Phys. Soc. (London) **89**, 987 (1966).

<sup>8</sup>M. Klein, G. K. Horton, and J. L. Feldman, Phys. Rev. **184**, 968 (1969).

<sup>9</sup>The specific heat measured is actually  $C_S$ , the specific heat of the solid in equilibrium with its vapor. The difference between  $C_S$  and  $C_p$  is small for neon—about 0.1% at the triple point.

<sup>10</sup>K. Clusius, P. Flubacher, U. Piesbergen, K. Schleich, and A. Z. Sperandio, Z. Naturforsch. **152**, 1 (1960).

<sup>11</sup>G. A. Cook, in *Argon, Helium, And The Rare Gases*, edited by G. A. Cook (Interscience, New York, 1961), p. 10.

<sup>12</sup>H. Fenichel and B. Serin, Phys. Rev. **142**, 490 (1966).

<sup>13</sup>C. H. Fagestroem and A. C. Hollis Hallet, in *Low Temperature Physics—LT 9*, edited by J. G. Daunt, D. O. Edwards, F. J. Milford, and M. Yaqub (Plenum, New York, 1965), p. 1092.

<sup>14</sup>S. S. Shinozaki and A. Arrott, Phys. Rev. **152**, 611 (1966).

<sup>15</sup>Cryocal, Inc., 1371 Avenue "E," Riviera Beach, Fla. 33404.

<sup>16</sup>The General Electric Co., Schenectady, N. Y.

<sup>17</sup>F. G. Brickwedde, H. van Dijk, M. Durieux, J. R. Clement, and J. K. Logan, *The 1958 Helium Four Scale of Temperatures*, Natl. Bur. Std. (US) Monograph No. 10 (U. S. GPO, Washington, D. C., 1958).

<sup>18</sup>E. Somoza, thesis (University of Cincinnati, 1968) (unpublished).

<sup>19</sup>W. H. Keesom, *Helium* (Elsevier, Amsterdam, 1942), p. 49.

<sup>20</sup>G. Ahlers and J. F. Macre, Rev. Sci. Instr. **37**, 962 (1966).

<sup>21</sup>Mound Laboratories, Miamisburg, Ohio, 45342.

<sup>22</sup>Guidline Instruments, Ltd., Smith Falls, Ontario, Canada.

<sup>23</sup>Keithley Instruments, 12415 Euclid Avenue, Cleveland, Ohio.

<sup>24</sup>Note that the  $^{22}\text{Ne}$  data for run I are missing. An error in the measuring procedure invalidated the  $^{22}\text{Ne}$  portion of this run.

<sup>25</sup>M. W. Zemansky, *Heat and Thermodynamics*, 4th

ed. (McGraw-Hill, New York, 1957).

<sup>26</sup>All these quantities have been measured (see Ref. 27) except for  $\chi_T$  for  $^{22}\text{Ne}$ . For this we have taken the values suggested in Ref. 27, which are taken to be 3.5% lower than the corresponding values for  $^{20}\text{Ne}$ .

<sup>27</sup>D. N. Batchelder, D. L. Losee, and R. O. Simmons, Phys. Rev. **162**, 767 (1967); D. N. Batchelder, Atomic Energy Commission Report No. C00-1198-296, 1965 (unpublished).

<sup>28</sup>P. Giguère and M. Boisvert, *Tables des Fonctions Thermodynamique de Debye* (Les Presses de l'Université Laval, Quebec, 1962).

<sup>29</sup>There is some controversy about the validity of this equation, although it is widely used. See Ref. 4 for a discussion of the equation.

<sup>30</sup>E. Somoza and H. Fenichel, in *Low Temperature Physics—LT 11*, edited by J. F. Allen, D. M. Finlayson, and D. M. McCall (University of St. Andrews Printing Dept., St. Andrews, Scotland, 1969), p. 549.

<sup>31</sup>No detailed analyses of vacancy contributions to the thermodynamic properties of solid neon have been published. For a discussion of vacancies in some of the heavier NGS see D. L. Losee and R. O. Simmons, Phys. Rev. **172**, 934 (1968); O. G. Peterson, D. N. Batchelder, and R. O. Simmons, Phil. Mag. **120**, 1193 (1965).

<sup>32</sup>T. H. K. Barron, in *Lattice Dynamics*, edited by R. F. Wallis (Pergamon, Oxford, 1964), p. 247.

<sup>33</sup>O. G. Peterson, D. N. Batchelder, and R. O. Simmons, Phys. Rev. **150**, 703 (1966).

<sup>34</sup>E. Grüneisen, in *Handbuch der Physik*, edited by H. Geiger and K. Scheel (Verlag-Springer, Berlin, 1926), Vol. 10, p. 1.

<sup>35</sup>H. H. Sample and C. A. Swenson, Phys. Rev. **158**, 188 (1967).

<sup>36</sup>T. H. K. Barron, Phil. Mag. **46**, 720 (1955).

<sup>37</sup>G. K. Horton and J. W. Leech, Proc. Phys. Soc. (London) **82**, 816 (1963).

<sup>38</sup>C. Feldman, J. L. Feldman, G. K. Horton, and M. L. Klein, Proc. Phys. Soc. (London) **90**, 1182 (1967).

<sup>39</sup>J. W. Leech and J. A. Reissland, Discussions Faraday Soc. **40**, 123 (1965).

<sup>40</sup>T. H. K. Barron and M. L. Klein, Proc. Phys. Soc. (London) **85**, 523 (1965).

<sup>41</sup>The slight difference between  $^{20}\text{Ne}$  and natural neon is neglected in this discussion.

<sup>42</sup>G. Leibfried and W. Ludwig, in *Solid State Physics*, edited by F. Seitz and D. Turnbull (Academic, New York, 1961), Vol. 12, p. 275.

<sup>43</sup>There is some confusion in the notation used in the literature for this anharmonic coefficient. The symbol  $A$  is used for the coefficient of Eqs. (9)–(12). However, the same symbol  $A$  is also used by some authors in the high-temperature expansion equation  $C_v^{\text{anh}} - C_v^{\text{h}}/3Nk = S^{\text{anh}} - S^{\text{h}}/3Nk = AT$ , Ref. 44. This latter  $A$  is actually the negative of the former. For a discussion of this see Sec. II of Ref. 45.

<sup>44</sup>See, for example, A. A. Maradudin, P. A. Flinn, and R. A. Coldwell-Horsfell, Ann. Phys. (N. Y.) **15**, 360 (1961); M. P. Tosi and F. G. Fumi, Phys. Rev.

131, 1458 (1963).

<sup>45</sup>D. M. T. Newsham, Phys. Rev. **152**, 841 (1966).

<sup>46</sup>J. Kuebler and M. P. Tosi, Phys. Rev. **137**, A1617 (1965).

<sup>47</sup>E. Somoza and H. Fenichel, J. Chem. Phys. **48**, 2382 (1968).

<sup>48</sup>R. H. Gupta and N. P. Gupta, Nuovo Cimento **66B**, 1 (1970).

<sup>49</sup>N. S. Gillis, N. R. Werthamer, and T. R. Koehler, Phys. Rev. **165**, 951 (1968).

<sup>50</sup>N. R. Werthamer, Am. J. Phys. **37**, 763 (1969).

<sup>51</sup>V. V. Goldman, G. K. Horton, and M. L. Klein, J. Low-Temp. Phys. **1**, 391 (1969).

<sup>52</sup>J. A. Leake, W. B. Daniels, J. Skalyo, Jr., B. C. Frazer, and G. Shirane, Phys. Rev. **181**, 1251 (1969).

PHYSICAL REVIEW B

VOLUME 3, NUMBER 10

15 MAY 1971

## Raman Scattering and Small-Angle X-Ray Scattering in $\text{KCl}_{1-x}\text{Br}_x$ <sup>†</sup>

Indira Nair and Charles T. Walker

*Department of Physics, Northwestern University, Evanston, Illinois 60201*

(Received 2 December 1970)

The Raman spectra of the mixed halide  $\text{KCl}_{1-x}\text{Br}_x$  were studied as a function of concentration. First-order Raman-active phonons of  $A_{1g}$  symmetry were observed at approximately 120 and 145  $\text{cm}^{-1}$  at  $x < 0.3$ . Above this concentration, the 120- $\text{cm}^{-1}$  mode disappeared, leaving the higher-frequency band only in the first-order spectrum. This band was found to shift linearly with concentration and the extrapolation of the straight-line fit intersects the pure-crystal axes at values close to that of the pure-crystal TO(X) phonon. At the KBr end of the concentration range, the first-order spectrum resembles the pure-crystal density of states. The first-order spectra of the  $T_{2g}$  symmetry were also studied. These reflect the pure-crystal density of states at both ends of the concentration range. The crystals were also investigated by small-angle x-ray scattering for evidence of clustering. No clusters smaller than  $(30)^3$  unit cells were found. Because of the comparable intensities of the first- and second-order spectra, it was not possible to arrive at perfectly conclusive results.

### I. INTRODUCTION

This paper describes the results of an investigation of the Raman spectra of  $\text{KCl}_{1-x}\text{Br}_x$  for  $1 \geq x \geq 0$ . Mixed crystals of alkali halides have been studied extensively by x-ray and thermodynamic techniques.<sup>1-6</sup> The results of these studies most relevant to the present work are the following: (a) KCl-KBr system forms a homogeneous series of continuous solid solutions at all temperatures.<sup>3</sup> (b) The system obeys Vegard's law, i. e., linear dependence of the lattice constants of solid solutions on composition,<sup>4</sup> the agreement being to within 0.08%. The optical phonons of  $\text{KCl}_{1-x}\text{Br}_x$  have been studied by Mitsuishi<sup>7</sup> using thin-film transmission measurements and by Fertel and Perry<sup>8</sup> from a Kramers-Kronig analysis of the reflectivity spectra. Mitsuishi finds a linear variation of the TO frequency with composition while the results of Fertel and Perry show a nonlinear variation.

Several theoretical models have been proposed to describe the behavior of phonons in mixed crystals.<sup>9</sup> The first such attempt by Matossi<sup>10</sup> considered a linear diatomic chain model of a 50-50 crystal  $AB_{1-x}C_x$  with nearest-neighbor force constants only. This model predicted two modes which are weakly Raman active or inactive depending upon whether the structure of the mixed crystal is peri-

odic or statistical, and one mode which is Raman active in either case. The virtual-crystal model of Langer,<sup>11</sup> in which all masses and force constants are taken as averages weighted by the mixed crystal composition, gives only qualitative results and predicts a linear variation of phonon frequency with composition. These models are one dimensional. However, the qualitative results are similar for one-, two-, and three-dimensional lattices.<sup>12</sup> Verleur and Barker<sup>13</sup> considered a model based on short-range clustering to account for the two-mode behavior of semiconductor mixed crystals. In their model, a one-mode behavior would result when the frequencies of the pure end members are close to each other. The random-element isodisplacement (REI) model of Chen, Shockley, and Pearson<sup>14</sup> considered essentially a unit cell containing one unit of  $AB_{1-x}C_x$  and then assumed randomness, i. e., each atom is subjected to forces produced by a statistical average of its neighbors and no effects of order are present. The Grüneisen constant enters the model calculations as a parameter, the force constants  $F_{AB}$  and  $F_{AC}$  at  $x = 0$  and  $x = 1$  are related to the optic frequencies of the end members AB and AC, and a third force constant  $F_{BC}$  is used as an adjustable parameter.

This model has been altered in the modified random-element isodisplacement (MREI) model of